

Strain engineering of Zeeman and Rashba effects in transition metal dichalcogenide nanotubes and their Janus variants: An ab initio study

Arpit Bhardwaj and Phanish Suryanarayana*

College of Engineering, Georgia Institute of Technology, Atlanta, GA 30332, USA

Abstract

We study the influence of mechanical deformations on the Zeeman and Rashba effects in synthesized transition metal dichalcogenide (TMD) nanotubes and their Janus variants from first principles. In particular, we perform symmetry-adapted density functional theory simulations with spin-orbit coupling to determine the variation in the Zeeman and Rashba splittings with axial and torsional deformations. We find significant splitting in molybdenum and tungsten nanotubes, for which the Zeeman splitting decreases with increase in strain, going to zero for large enough tensile/shear strains, while the Rashba splitting coefficient increases linearly with shear strain, while being zero for all tensile strains, a consequence of the inversion symmetry remaining unbroken. In addition, the Zeeman splitting is relatively unaffected by nanotube diameter, whereas the Rashba coefficient decreases with increase in diameter. Overall, mechanical deformations represent a powerful tool for spintronics in TMD nanotubes as well as their Janus variants.

I. INTRODUCTION

Transition metal dichalcogenide (TMD) nanotubes are 1D materials of the form MX_2 , where M and X represent a transition metal and chalcogen, respectively¹. They represent the most diverse group of nanotubes, there being 38 transition metals and 3 chalcogens, resulting in a total of 114 possible combinations. Of these, around 12 have already been synthesized, which represents a significant fraction of the total number of experimentally realized nanotubes, and the most in any group¹⁻³. The number of such nanotubes doubles when considering their Janus variants⁴ — nanotubes of the form MXY , where Y represents a chalcogen that is distinct from X — of which WSSe has recently been synthesized⁵.

TMD nanotubes and their Janus variants demonstrate varying electronic properties, ranging from semiconducting⁶⁻¹⁰ to metallic¹⁰⁻¹² to superconducting^{13,14}. Notably, these properties can be tuned/engineered by a number of mechanisms, including mechanical deformation^{10,15-20}, electric field^{21,22}, temperature^{13,14}, chirality/radius^{7,23-27}, and defects^{28,29}. This makes the nanotubes ideally suited for various technological applications, including mechanical sensors^{20,30,31}, nanoelectromechanical (NEMS) devices^{19,32,33}, biosensors³⁴, photodetectors^{20,35-42}, and superconductive materials^{13,14}. However, the potential for TMD and Janus TMD nanotubes (and nanotubes in general) to be used in spintronic applications has not been studied heretofore, particularly in the context of first principles calculations.

Spintronics or spin electronics refers to the exploitation of both spin and the electronic charge in solid state devices⁴³. In this context, the Zeeman and Rashba effects are of particular interest, both being relativistic effects arising from spin-orbit coupling (SOC). In particular, the Zeeman and Rashba effects result in splitting of the electronic bands along the energy and wavevector axes, respectively, of particular importance being those at the valence band maximum (VBM) and the conduction band minimum (CBM). These effects have been studied in TMD monolayers and their Janus variants not only experimentally⁴⁴⁻⁴⁶, but also theoretically using ab initio Kohn-Sham density functional theory (DFT) calculations^{43,47,48}. In addition, the effect of strain on the Zeeman and Rashba splittings has been studied in Janus TMD bilayers⁴⁷ and their heterostructures⁴⁹ using DFT. However, there have been no such studies for TMD and Janus TMD nanotubes (and nanotubes in general), which

provides the motivation for the current investigation.

In this work, we study the influence of mechanical deformations on the Zeeman and Rashba effects in the synthesized TMD nanotubes and their Janus variants using Kohn-Sham DFT calculations. In particular, we perform symmetry-adapted DFT simulations with SOC to determine the variation in the Zeeman and Rashba splittings with axial and torsional deformations. We find significant splitting for the nanotubes having the transition metal as either molybdenum or tungsten. In particular, axial and torsional deformations can be used to vary the Zeeman splitting, while torsional deformations can be used to introduce and vary the Rashba splitting, making the nanotubes particularly well-suited for spintronics applications.

The remainder of this manuscript is organized as follows. In Section II, we list the standard and Janus TMD nanotubes studied and describe the symmetry-adapted Kohn-Sham DFT simulations for the calculation of the Zeeman and Rashba splittings. Next, we present and discuss the results of the simulations in Section III. Finally, we provide concluding remarks in Section IV.

II. SYSTEMS AND METHODS

We start by considering the TMD nanotubes that have been synthesized¹⁻³: {MoS₂, MoSe₂, MoTe₂, WS₂, WSe₂, WTe₂, NbS₂, NbSe₂, TaS₂, TiS₂, TiSe₂, HfS₂, and ZrS₂}. Since we have found that spin-orbit coupling (SOC) does not cause any splitting in the nanotubes: {NbS₂, NbSe₂, TaS₂, TiS₂, TiSe₂, HfS₂, and ZrS₂}, we henceforth consider the remaining TMD nanotubes: {MoS₂, MoSe₂, MoTe₂, WS₂, WSe₂, WTe₂}, as well as their Janus variants with the heavier chalcogen on the outside: {MoSSe, MoSTe, MoSeTe, WSSe, WSTe, WSeTe}, all with 2H-t symmetry. We consider their armchair configurations, since the results remain unchanged for the zigzag configuration, in agreement with previous observations for SOC in the MoS₂ nanotube⁵⁰. The diameters of the TMD nanotubes are chosen to be commensurate with those synthesized, and the diameters of the Janus TMD nanotubes are set to DFT-calculated equilibrium values (Table I). The axial and torsional deformations considered are also commensurate with those in experiments^{19,33,51-53}. Indeed, through phonon

calculations using ABINIT⁵⁴, we have verified that the monolayer counterparts are stable at the largest tensile/shear strains (Supplementary Material), which suggests the stability of the nanotubes at the chosen strains, as curvature effects on the phonon spectrum are expected to be minor at the relatively large diameters of the nanotubes.

Table I: Diameters of the TMD nanotubes^{55,56} and their Janus variants^{10,57}.

Material	Diameter (nm)	Material	Diameter (nm)	Material	Diameter (nm)
MoS ₂	3.2	MoSe ₂	3.2	MoTe ₂	3.6
WS ₂	3.2	WSe ₂	3.2	WTe ₂	3.5
MoSSe	8.4	MoSTe	3.8	MoSeTe	6.6
WSSe	8.8	WSTe	3.8	WSeTe	6.6

We perform Kohn-Sham DFT simulations using the Cyclix-DFT⁵⁸ feature in the state-of-the-art real-space code SPARC^{59–61}. In particular, we perform symmetry-adapted calculations that exploit the cyclic and/or helical symmetry in the system to reduce the Kohn-Sham problem to the unit cell/fundamental domain with minimal number of atoms^{58,62}, e.g., the fundamental domain for the chosen nanotubes contains only 3 atoms, i.e., 1 metal and 2 chalcogen atoms (Fig. 1). This reduction due to symmetry can be exploited even on the application of axial and/or torsional deformations, tremendously lowering the computational expense, given that DFT calculations scale cubically with system size, making otherwise impractical calculations routine, e.g., a 8.5 nm diameter MoSSe nanotube with an external twist of 6×10^{-4} rad/bohr has 219,888 atoms in the simulation domain when employing periodic boundary conditions, a system size that is impractical even with state-of-the-art approaches⁶³. Cyclix-DFT is now a mature open source feature in SPARC, having been verified by comparisons with established DFT codes⁵⁸, and ability to make accurate predictions in diverse physical applications^{10,55–57,64–67}.

In all simulations, we employ the Perdew–Burke–Ernzerhof (PBE)⁶⁹ exchange-correlation functional, and optimized norm-conserving Vanderbilt (ONCV)⁷⁰ pseudopotentials with non-linear core correction (NLCC) and SOC from the PseudoDojo collection⁷¹. The equilibrium

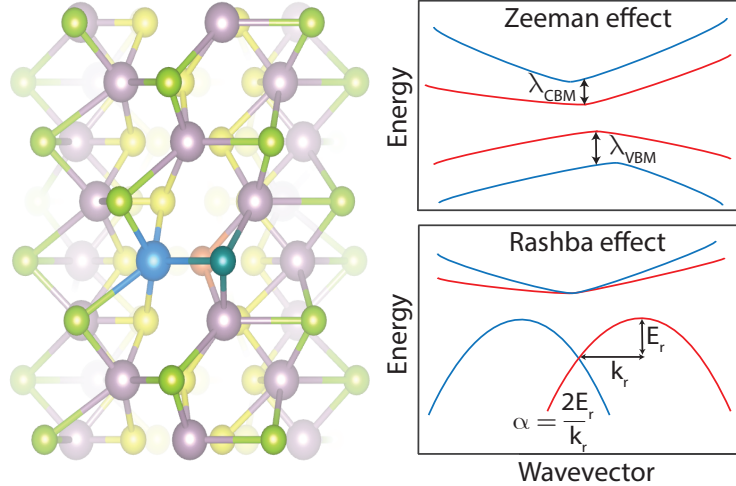


Figure 1: Left: Illustration of a Janus TMD nanotube subject to both axial and torsional deformations, with the three fundamental domain atoms colored blue, orange, and dark green (structural model generated using VESTA⁶⁸). Right: Illustration of the Zeeman and Rashba splittings in the electronic band structure, with λ_{VBM} and λ_{CBM} denoting the Zeeman split at the valence band maximum (VBM) and conduction band minimum (CBM), respectively, and α representing the Rashba splitting coefficient.

geometry of the nanotubes (Supplementary Material) is in very good agreement with previous DFT calculations^{8,16,72–75}, and the equilibrium geometry of the corresponding monolayers (Supplementary Material) is in very good agreement with experiments^{76–79} as well as DFT calculations^{16,17,80–82}, verifying the accuracy of the chosen pseudopotential and exchange-correlation functional. Though more advanced and expensive exchange-correlation functionals such as hybrid generally provide better spectral properties, this is not always the case, e.g., Janus TMD monolayers⁵⁷, motivating the choice of PBE exchange-correlation here, as done in previous works for such systems^{8,72,74,75,81}. The numerical parameters in the Cyclix-DFT simulations, including grid spacing for real-space discretization, grid spacing for Brillouin zone integration, vacuum in the radial direction, and structural relaxation tolerances, are chosen such that the Zeeman splitting values and Rashba coefficients are converged to within 0.01 eV and 0.01 eV Å, respectively. This translates to an accuracy of 10^{-4} Ha/atom in the ground state energy.

III. RESULTS AND DISCUSSION

We now use the aforescribed framework to study the effect of axial and torsional deformations on the Zeeman and Rashba splittings in the molybdenum and tungsten TMD nanotubes and their Janus variants. In the results presented here, the axial strain (ε) is defined as the change in nanotube length divided by its original length; the shear strain (γ) is defined as the product of the nanotube radius with the applied twist per unit length; the Zeeman splitting (λ_{VBM}) corresponds to the valence band maximum (VBM), where the effect is significantly more pronounced ($\sim 5x$ larger) than the conduction band minimum (CBM) (Supplementary Material); and the Rashba splitting coefficient (α) corresponds to the VBM, calculated at the zero wavevector in the axial direction. All the data can be found in the Supplementary Material.

In Fig. 2, we present the variation in the Zeeman splitting with tensile and shear strains. We observe that the Zeeman splitting in the undeformed state is significant, being comparable to the monolayer counterparts⁴³, with the WTe₂ and MoS₂/MoSTe nanotubes having the largest and smallest values of $\lambda_{\text{VBM}} = 489$ and ~ 146 meV, respectively. In addition, the splitting decreases with increase in tensile strains, going to zero for large enough strains. A similar behavior is also observed for shear strains, other than for the MoSe₂, WS₂, WSSe, and WSTe nanotubes, where the splitting remains unaffected by the torsional deformations. Such a decrease in the Zeeman splitting values upon the application of biaxial strains has been observed for Janus TMD bilayers⁴⁷. Note that the values for the Janus TMD nanotubes are generally in between their parent TMDs. Note also that the sudden jumps in the Zeeman splitting values are a consequence of the VBM location shifting to a different wavevector.

In Fig 3, we present the variation in the Rashba coefficient with shear strain. Unlike torsional deformations, axial deformations do not break the inversion symmetry of the nanotube, and therefore the Rashba effect remains absent⁸³. We observe that the Rashba coefficient increases linearly with shear strain — average coefficient of determination of linear regression over all the materials is 0.97 — reaching significantly large values that are comparable to those for Janus TMD monolayers⁴⁷, systems where we have found the Rashba effect to be insensitive to shear strains. Indeed, the Rashba effect is not observed in TMD monolayers

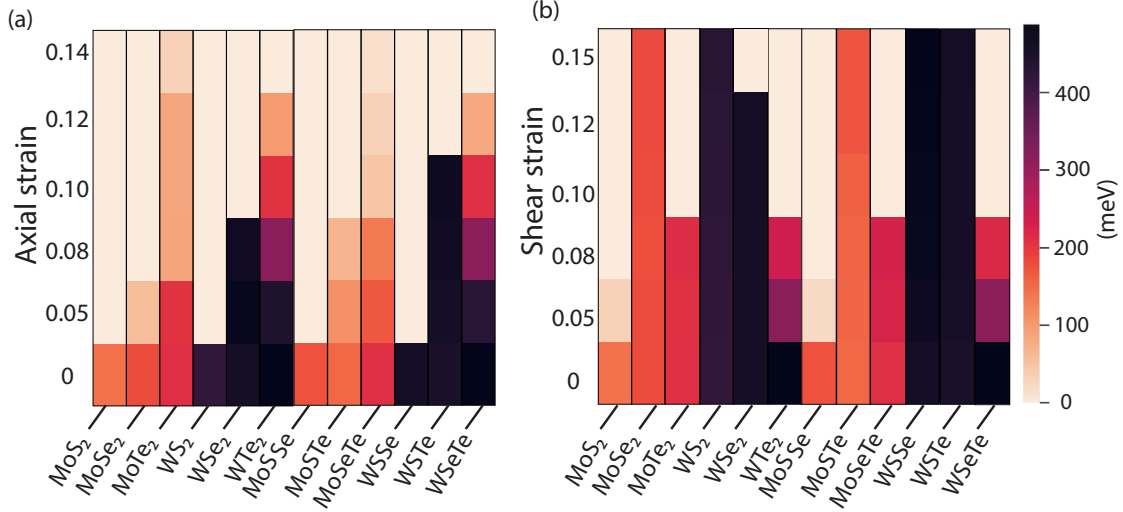


Figure 2: Variation in the Zeeman splitting (λ_{VBM}) for the molybdenum and tungsten TMD nanotubes and their Janus variants with (a) tensile strain (ε) and (b) shear strain (γ). The tensile and shear strains result from the application of axial and torsional deformations, respectively.

due to the presence of inversion symmetry. At the largest shear strain of $\gamma = 0.15$, the largest and smallest Rashba coefficient values of $\alpha = 0.78$ and 0.20 eV \AA occur for the WTe₂ and MoS₂ nanotubes, respectively, whose undeformed configurations also have the largest and smallest Zeeman splitting, respectively. However, this correlation is not generally true, e.g., MoTe₂ has one of the smallest Zeeman splitting of $\lambda_{\text{VBM}} = 213 \text{ meV}$ for the undeformed nanotube, whereas it has one of the largest Rashba coefficient of $\alpha = 0.65 \text{ eV \AA}$ for the maximum shear strained tube ($\gamma = 0.15$). Note that the values for the Janus TMD nanotubes are generally in between their parent TMDs.

To understand the effect of the nanotube diameter on the results obtained, we now consider the nanotubes that demonstrate the largest Zeeman and Rashba effects, i.e., WSe₂, WSeTe, and WTe₂, with diameters spanning the range $\sim 2 - 10 \text{ nm}$. In Fig. 4, we present the variation in the Zeeman splitting and Rashba coefficient with the diameter, while considering the unstrained and largest shear strain ($\gamma = 0.15$) configurations, respectively. We observe that the Zeeman splitting values remain relatively unchanged, increasing ever so slightly with diameter — around 1% over the entire diameter range — approaching the flat

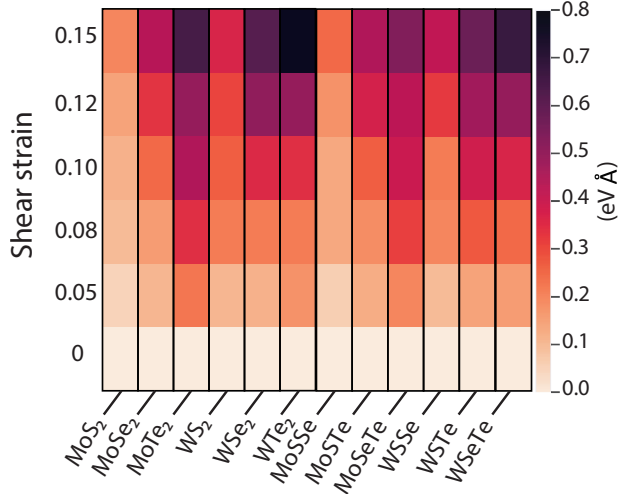


Figure 3: Variation in the Rashba splitting coefficient (α) for the molybdenum and tungsten TMD nanotubes and their Janus variants with shear strain (γ). The shear strain results from the application of torsional deformations.

sheet values of $\lambda_{\text{VBM}} = 463, 473,$ and 493 meV for WSe_2 , WSeTe , and WTe_2 , respectively⁴³. In addition, the Rashba coefficient decreases significantly with increase in diameter, e.g., the value for WTe_2 reduces from $\alpha = 0.83$ eV Å at a diameter of 2 nm to $\alpha = 0.73$ eV Å at a diameter of 9 nm, expectedly heading towards the zero value for the flat sheet configuration.

The results presented here clearly demonstrate that mechanical deformations can be used to engineer the Zeeman and Rashba splittings in molybdenum and tungsten TMD nanotubes as well as their Janus variants, making them a powerful tool for spintronics applications. In particular, the Zeeman effect is especially significant for the undeformed nanotubes, becoming progressively smaller and even disappearing with increase in axial/shear strains, and the Rashba effect can be introduced through torsional deformations — break the inversion symmetry of the system — becoming especially significant as the shear strain increases.

IV. CONCLUDING REMARKS

In this work, we have studied the strain engineering of Zeeman and Rashba effects in synthesized TMD nanotubes and their Janus variants using first principles DFT simulations. In

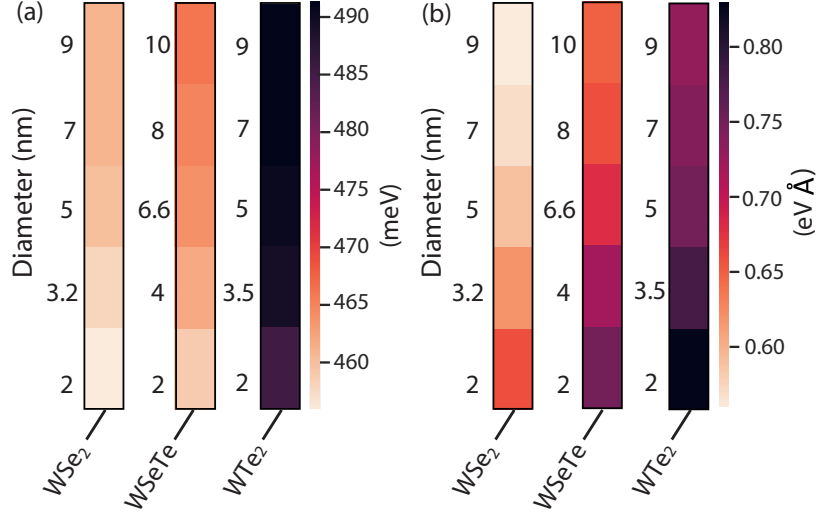


Figure 4: Variation in the (a) Zeeman splitting (λ_{VBM}) and (b) Rashba coefficient (α) with diameter. The Zeeman splitting corresponds to undeformed nanotube, while the Rashba coefficient corresponds to the maximum shear strained ($\gamma = 0.15$) nanotube.

particular, we have performed symmetry-adapted Kohn-Sham calculations with spin-orbit coupling to determine the effect of axial and torsional deformations on the Zeeman and Rashba splittings in the electronic band structure. We have found that there is significant splitting in the molybdenum and tungsten nanotubes, for which the Zeeman splitting decreases with increase in tensile/shear strain, reaching zero for large enough strains, while the Rashba splitting coefficient increases linearly with shear strain, while being zero for all axial deformations, a consequence of the inversion symmetry remaining unbroken. In addition, the Zeeman splitting is relatively unaffected by the nanotube diameter, whereas the Rashba coefficient decreases with increase in diameter. Though the current study has been restricted to TMD nanotubes and their Janus variants, other nanotubes are expected to demonstrate similar behavior, particularly those with heavy chemical elements. Overall, mechanical deformations represent a powerful tool for spintronics applications using nanotubes.

ACKNOWLEDGEMENTS

The authors gratefully acknowledge the support of the Clifford and William Greene, Jr. Professorship. This research was also supported by the supercomputing infrastructure provided by Partnership for an Advanced Computing Environment (PACE) through its Hive (U.S. National Science Foundation (NSF) through grant MRI-1828187) and Phoenix clusters at Georgia Institute of Technology, Atlanta, Georgia.

* phanish.suryanarayana@ce.gatech.edu

- ¹ Rao C N R and Nath M 2003 Inorganic nanotubes *Advances In Chemistry: A Selection of CNR Rao's Publications (1994–2003)* (World Scientific) pp 310–333
- ² Tenne R 2003 *Angewandte Chemie International Edition* **42** 5124–5132
- ³ Serra M, Arenal R and Tenne R 2019 *Nanoscale* **11** 8073–8090
- ⁴ Yagmurcukardes M, Qin Y, Ozen S, Sayyad M, Peeters F M, Tongay S and Sahin H 2020 *Applied Physics Reviews* **7** 011311
- ⁵ Sreedhara M B, Miroshnikov Y, Zheng K, Houben L, Hettler S, Arenal R, Pinkas I, Sinha S S, Castelli I E and Tenne R 2022 *Journal of the American Chemical Society*
- ⁶ Seifert G, Terrones H, Terrones M, Jungnickel G and Frauenheim T 2000 *Physical Review Letters* **85** 146
- ⁷ Seifert G, Terrones H, Terrones M, Jungnickel G and Frauenheim T 2000 *Solid State Communications* **114** 245–248
- ⁸ Mikkelsen A E G, Bølle F T, Thygesen K S, Vegge T and Castelli I E 2021 *Physical Review Materials* **5** 014002
- ⁹ Tao L, Zhang Y Y, Sun J, Du S and Gao H J 2018 *Chinese Physics B* **27** 076104
- ¹⁰ Bhardwaj A and Suryanarayana P 2022 *The European Physical Journal B* **95** 1–9
- ¹¹ Seifert G, Terrones H, Terrones M and Frauenheim T 2000 *Solid State Communications* **115** 635–638

- ¹² Enyashin A N, Shein I R, Medvedeva N I and Ivanovskii A L 2005 *Internet Electronic Journal of Molecular Design* **4** 316–328
- ¹³ Nath M, Kar S, Raychaudhuri A K and Rao C N R 2003 *Chemical Physics Letters* **368** 690–695
- ¹⁴ Tsuneta T, Toshima T, Inagaki K, Shibayama T, Tanda S, Uji S, Ahlskog M, Hakonen P and Paalanen M 2003 *Current Applied Physics* **3** 473–476
- ¹⁵ Zibouche N, Ghorbani-Asl M, Heine T and Kuc A 2014 *Inorganics* **2** 155–167
- ¹⁶ Li W, Zhang G, Guo M and Zhang Y W 2014 *Nano Research* **7** 518–527
- ¹⁷ Wang Y Z, Huang R, Wang X Q, Zhang Q F, Gao B L, Zhou L and Hua G 2016 *Chalcogenide Letters* **13** 301–307
- ¹⁸ Lu P, Wu X, Guo W and Zeng X C 2012 *Physical Chemistry Chemical Physics* **14** 13035–13040
- ¹⁹ Levi R, Garel J, Teich D, Seifert G, Tenne R and Joselevich E 2015 *ACS Nano* **9** 12224–12232
- ²⁰ Oshima S, Toyoda M and Saito S 2020 *Physical Review Materials* **4** 026004
- ²¹ Wang Y Z, Wang B L, Zhang Q F, Huang R, Gao B L, Kong F J and Wang X Q 2014 *Chalcogenide Letters* **11** 493–502
- ²² Zibouche N, Philipsen P and Kuc A 2019 *The Journal of Physical Chemistry C* **123** 3892–3899
- ²³ Ivanovskaya V V, Enyashin A N, Medvedeva N I, Makurin Y N and Ivanovskii A L 2003 *Internet Electronic Journal of Molecular Design* **2** 499–510
- ²⁴ Gao B L, Ke S H, Song G, Zhang J, Zhou L, Li G N, Liang F, Wang Y and Dang C 2017 *Journal of Alloys and Compounds* **695** 2751–2756
- ²⁵ Yin D, Wu M, Yang Y, Cen W and Fang H 2016 *Physica E: Low-dimensional Systems and Nanostructures* **84** 196–201
- ²⁶ Zibouche N, Kuc A and Heine T 2012 *The European Physical Journal B* **85** 49
- ²⁷ Ansari R, Malakpour S, Faghihnasiri M and Sahmani S 2015 *Superlattices and Microstructures* **82** 188–200
- ²⁸ Tal O, Remskar M, Tenne R and Haase G 2001 *Chemical Physics Letters* **344** 434–440
- ²⁹ Li N, Lee G, Jeong Y H and Kim K S 2015 *The Journal of Physical Chemistry C* **119** 6405–6413
- ³⁰ Li B L, Wang J, Zou H L, Garaj S, Lim C T, Xie J, Li N B and Leong D T 2016 *Advanced Functional Materials* **26** 7034–7056

- ³¹ Sorkin V, Pan H, Shi H, Quek S Y and Zhang Y W 2014 *Critical Reviews in Solid State and Materials Sciences* **39** 319–367
- ³² Yudilevich D, Levi R, Nevo I, Tenne R, Ya'akovovitz A and Joselevich E 2018 *ICME* 1–4
- ³³ Divon Y, Levi R, Garel J, Golberg D, Tenne R, Ya'akovovitz A and Joselevich E 2017 *Nano Letters* **17** 28–35
- ³⁴ Barua S, Dutta H S, Gogoi S Devi R and Khan R 2017 *ACS Applied Nano Materials* **1** 2–25
- ³⁵ Unalan H E, Yang Y, Zhang Y, Hiralal P, Kuo D, Dalal S, Butler T, Cha S N, Jang J E, Chremmou K *et al.* 2008 *IEEE Transactions on Electron Devices* **55** 2988–3000
- ³⁶ Zhang C, Wang S, Yang L, Liu Y, Xu T, Ning Z, Zak A, Zhang Z, Tenne R and Chen Q 2012 *Applied Physics Letters* **100** 243101
- ³⁷ Zhang Y J, Ideue T, Onga M, Qin F, Suzuki R, Zak A, Tenne R, Smet J H and Iwasa Y 2019 *Nature* **570** 349–353
- ³⁸ Tang Z K, Wen B, Chen M and Liu L M 2018 *Advanced Theory and Simulations* **1** 1800082
- ³⁹ Xie S, Jin H, Wei Y and Wei S 2021 *Optik* **227** 166105
- ⁴⁰ Ju L, Liu P, Yang Y, Shi L, Yang G and Sun L 2021 *Journal of Energy Chemistry* **61** 228–235
- ⁴¹ Ju L, Qin J, Shi Land Yang G, Zhang J and Sun L 2021 *Nanomaterials* **11** 705
- ⁴² Zhang S, Jin H, Long C, Wang T, Peng R, Huang B and Dai Y 2019 *Journal of Materials Chemistry A* **7** 7885–7890
- ⁴³ Cheng Y C, Zhu Z Y, Tahir M and Schwingenschlögl U 2013 *Europhysics Letters* **102** 57001
- ⁴⁴ Larentis S, Movva H C P, Fallahazad B, Kim K, Behroozi A, Taniguchi T, Watanabe K, Banerjee S K and Tutuc E 2018 *Physical Review B* **97** 201407
- ⁴⁵ Li Q, Zhao X, Deng L, Shi Z, Liu S, Wei Q, Zhang L, Cheng Y, Zhang L, Lu H *et al.* 2020 *ACS Nano* **14** 4636–4645
- ⁴⁶ Jiang C, Liu F, Cuadra J, Huang Z, Li K, Rasmita A, Srivastava A, Liu Z and Gao W B 2017 *Nature Communications* **8** 802
- ⁴⁷ Rezavand A and Ghobadi N 2021 *Physica E: Low-dimensional Systems and Nanostructures* **132** 114768
- ⁴⁸ Chen J, Wu K, Ma H, Hu W and Yang J 2020 *RSC Advances* **10** 6388–6394
- ⁴⁹ Rezavand A and Ghobadi N 2022 *Journal of Magnetism and Magnetic Materials* **544** 168721

- ⁵⁰ Milivojevic M, Dmitrovic S, Damnjanovic M and Vukovic T 2020 *The Journal of Physical Chemistry C* **124** 11141–11149
- ⁵¹ Nagapriya K S, Goldbart O, Kaplan-Ashiri I, Seifert G, Tenne R and Joselevich E 2008 *Physical Review Letters* **101** 195501
- ⁵² Kaplan-Ashiri I and Tenne R 2007 *Journal of Cluster Science* **18** 549–563
- ⁵³ Kaplan-Ashiri I, Cohen S R, Gartsman K, Ivanovskaya V, Heine T, Seifert G, Wiesel I, Wagner H D and Tenne R 2006 *Proceedings of the National Academy of Sciences* **103** 523–528
- ⁵⁴ Gonze X, Beuken J M, Caracas R, Detraux F, Fuchs M, Rignanese G M, Sindic L, Verstraete M, Zerah G, Jollet F *et al.* 2002 *Computational Materials Science* **25** 478–492
- ⁵⁵ Bhardwaj A, Sharma A and Suryanarayana P 2021 *Nanotechnology* **32** 28LT02
- ⁵⁶ Bhardwaj A, Sharma A and Suryanarayana P 2021 *Nanotechnology* **32** 47LT01
- ⁵⁷ Bhardwaj A and Suryanarayana P 2022 *The European Physical Journal B* **95** 1–8
- ⁵⁸ Sharma A and Suryanarayana P 2021 *Physical Review B* **103** 035101
- ⁵⁹ Xu Q, Sharma A, Comer B, Huang H, Chow E, Medford A J, Pask J E and Suryanarayana P 2021 *SoftwareX* **15** 100709
- ⁶⁰ Zhang B, Jing X, Xu Q, Kumar S, Sharma A, Erlandson L, Sahoo S J, Chow E, Medford A J, Pask J E *et al.* 2023 *arXiv preprint arXiv:2305.07679*
- ⁶¹ Ghosh S and Suryanarayana P 2017 *Computer Physics Communications* **212** 189–204
- ⁶² Ghosh S, Banerjee A S and Suryanarayana P 2019 *Physical Review B* **100** 125143
- ⁶³ Gavini V, Baroni S, Blum V, Bowler D R, Buccheri A, Chelikowsky J R, Das S, Dawson W, Delugas P, Dogan M *et al.* 2022 *arXiv preprint arXiv:2209.12747*
- ⁶⁴ Codony D, Arias I and Suryanarayana P 2021 *Physical Review Materials* **5** L030801
- ⁶⁵ Kumar S, Codony D, Arias I and Suryanarayana P 2021 *Nanoscale* **13** 1600–1607
- ⁶⁶ Kumar S and Suryanarayana P 2020 *Nanotechnology* **31** 43LT01
- ⁶⁷ Bhardwaj A and Suryanarayana P 2023 *The European Physical Journal B* **96** 36
- ⁶⁸ Momma K and Izumi F 2008 *Journal of Applied Crystallography* **41** 653–658
- ⁶⁹ Perdew J P, Burke K and Ernzerhof M 1996 *Physical Review Letters* **77** 3865
- ⁷⁰ Hamann D R 2013 *Physical Review B* **88** 085117

- ⁷¹ van Setten M J, Giantomassi M, Bousquet E, Verstraete M J, Hamann D R, Gonze X and Rignanese G M 2018 *Computer Physics Communications* **226** 39–54
- ⁷² Chang C H, Fan X, Lin S H and Kuo J L 2013 *Physical Review B* **88** 195420
- ⁷³ Luo Y F, Pang Y, Tang M, Song Q and Wang M 2019 *Computational Materials Science* **156** 315–320
- ⁷⁴ Wang Y Z, Huang R, Gao B L, Hu G, Liang F and Ma Y L 2018 *Chalcogenide Letters* **15** 535–543
- ⁷⁵ Bølle F T, Mikkelsen A E G, Thygesen K S, Vegge T and Castelli I E 2021 *npj Computational Materials* **7** 1–8
- ⁷⁶ Klots A R, Newaz A K M, Wang B, Prasai D, Krzyzanowska H, Lin J, Caudel D, Ghimire N J, Yan J, Ivanov B L *et al.* 2014 *Scientific Reports* **4** 1–7
- ⁷⁷ Ugeda M M, Bradley A J, Shi S F, Felipe H, Zhang Y, Qiu D Y, Ruan W, Mo S K, Hussain Z, Shen Z X *et al.* 2014 *Nature Materials* **13** 1091–1095
- ⁷⁸ Hill H M, Rigosi A F, Rim K T, Flynn G W and Heinz T F 2016 *Nano Letters* **16** 4831–4837
- ⁷⁹ Lu A Y, Zhu H, Xiao J, Chuu C P, Han Y, Chiu M H, Cheng C C, Yang C W, Wei K H, Yang Y *et al.* 2017 *Nature Nanotechnology* **12** 744–749
- ⁸⁰ Hastrup S, Strange M, Pandey M, Deilmann T, Schmidt P S, Hinsche N F, Gjerding M N, Torelli D, Larsen P M, Riis-Jensen A C *et al.* 2018 *2D Materials* **5** 042002
- ⁸¹ Shi W and Wang Z 2018 *Journal of Physics: Condensed Matter* **30** 215301
- ⁸² Zhao W, Li Y, Duan W and Ding F 2015 *Nanoscale* **7** 13586–13590
- ⁸³ Naaman R and Waldeck D H 2012 *The Journal of Physical Chemistry Letters* **3** 2178–2187